

439

~~2074~~

Library, Lm. 9 R

TECHNICAL MEMORANDUMS

NATIONAL ADVISORY COMMITTEE FOR AERONAUTICS

No. 675

CALCULATION OF POTENTIAL FLOW PAST AIRSHIP BODIES IN YAW

By I. Lotz

Ingenieur-Archiv, Vol. II, 1931

1.1

1.3.1

Washington  
July, 1932

NATIONAL ADVISORY COMMITTEE FOR AERONAUTICS

TECHNICAL MEMORANDUM NO. 675

CALCULATION OF POTENTIAL FLOW PAST AIRSHIP BODIES IN YAW\*

By I. Lotz

The calculation of the potential flow past an airship in yaw is accomplished, according to Von Karman, by dividing the air stream into a flow parallel to the airship axis and one perpendicular to it, after which the potential flow about the solid of rotation exposed in axial direction can then be determined by a method suggested by Rankine. The axis of the body is superposed by sources and sinks and the intensity so defined that the closed stream surface formed by superposition of parallel flow on this source-sink flow is coincident with the surface of the solid. Von Karman (reference 1) pursued an analogous method for defining the potential set up by the lateral flow. He disposes dipolars\*\* on the axis, so that the intensity of this superposition is again defined by the postulate that for the fluid motion, produced by superposition of parallel and dipolar flow, the surface of the solid is stream surface. Both problems yield integral equations. For approximate solution, he substituted a definite number of pieces with constant superposition for the continuous superposition. A numerical calculation of examples according to this method revealed certain difficulties for solids in yaw with not very slender bows, which finally prompted the use of sources and sinks on the surface of the solid instead of dipolars on the axis, and to compute the field of flow by this <sup>means</sup> agency. The experiences collected from the calculations and which should prove useful for other similar problems, form the subject of this report.

---

\*Zur Berechnung der Potentialströmung um quergestellte Luftschiffkörper. Ingenieur-Archiv, Vol. II, 1931, pp. 507-527.

\*\*On Dipolars and Their Fields of Flow. See Hütte, Vol. I, 26th edition, p. 364.

## I. AXIAL SUPERPOSITION

## A. Partially Constant Dipolar Superposition

The axis of the airship is assumed to coincide with axis  $x$ , counted from the bow. Cylindrical coordinates are introduced so that

$$z = r \cos \varphi, \quad y = r \sin \varphi \quad (\text{Fig. 1.})$$

The solid itself, of length  $l$  is assumed given by its meridian curve  $r(x)$ .

The normal velocities induced on the surface by the parallel flow in <sup>the</sup> direction of <sup>the</sup> negative axis  $z$ , are proportionate to  $\cos \varphi$ . Since dipoles lying on the axis of the solid also set up on the surface of the solid normal velocities proportionate to  $\cos \varphi$ , ~~the~~ angle  $\varphi$  does not appear in the integral equation defining dipolar motion  $\mu$ . This equation rests, as already stated, on the premise that the surface is <sup>a</sup>stream surface, so that on it the normal velocity, composed of <sup>the</sup> dipolar motion and <sup>the</sup> component set up by the flow, disappears. Designating the point of the axis carrying the superposition by  $\xi^*$ , expressing  $\frac{dr}{dx} = r'$  and  $W$  = velocity of air flow, this equation for the adherence of flow to a parallel of latitude with abscissa  $x$  reads as

$$\begin{aligned}
 & - \int_0^l \frac{\mu(\xi) d\xi}{\sqrt{r^2 + (x - \xi)^2}^3} + 3 r^2 \int_0^l \frac{\mu(\xi) d\xi}{\sqrt{r^2 + (x - \xi)^2}^5} \\
 & - 3 r r' \int_0^l \frac{\mu(\xi) (x - \xi) d\xi}{\sqrt{r^2 + (x - \xi)^2}^5} = 4 \pi W \quad (1)
 \end{aligned}$$

It is known, and Karman also pointed it out in his summary, that exact substitution of the body by a superposition on the axis of rotation is possible only "when the analytical continuation of the potential function free of singularities in the outer space of the solid can be extended to the axis of symmetry without encountering singu-

---

\*The zero point of  $\xi$  coincides with that for  $x$ .

lar points." Since the question of when or when not this continuance is possible, has never been answered, numerical calculations are apt to have disagreeable surprises in store.\*

With  $n$  <sup>interval</sup> spaces of constant <sup>doublet</sup> dipolar distribution the flow adheres only in  $n$  points (control points) of the meridian curve; that means on  $n$  circles of the body periphery. (Fig. 2.) The result is an  $n$  system of linear equations for the  $n$  unknown dipolar intensities  $\mu_v$ . With the  $v$ th dipol space reaching from  $\xi_v$  to  $\xi_{v+1}$  (fig. 3), the control point  $x$  (reference 1) for flow\*\* adherence is expressed as

$$\sum_{v=1}^n \mu_v [\Delta g_v + r' \Delta f_v] = 4 \pi r^2 W \quad (2)$$

whereby

$$\left. \begin{aligned} \Delta g_v &= g(x, \xi_v) - g(x, \xi_{v+1}), \\ \Delta f_v &= f(x, \xi_v) - f(x, \xi_{v+1}), \end{aligned} \right\} \quad (3)$$

where

$$\left. \begin{aligned} g(x, \xi) &= \cos \vartheta (2 - \cos^2 \vartheta), \\ f(x, \xi) &= \sin^3 \vartheta \end{aligned} \right\} \quad (4)$$

with

$$\tan \vartheta = \frac{r}{x - \xi} \quad (\text{Fig. 3.})$$

Karman has computed the functions  $g$  and  $f$  and they appear as dependent on  $\frac{x - \xi}{r}$ . For point  $x = 0$ ,  $r = 0$  equation (2) becomes

$$\frac{1}{2} \sum_{v=1}^n \mu_v \left( \frac{1}{\xi_{v+1}^2} - \frac{1}{\xi_v^2} \right) - m \sum_{v=1}^n \mu_v \left( \frac{1}{\xi_{v+1}^3} - \frac{1}{\xi_v^3} \right) = 4 \pi W \quad (5)$$

where  $m = \lim_{\substack{x \rightarrow 0 \\ r \rightarrow 0}} (r r')$

---

\*In the Jablonowski Prize Essay, 1914, G. Herglotz treated a similar problem: Analytical continuance of potential into the inside of the adhering masses, although the fundamental difference of the problems makes it impossible to expect any explanation.

\*\*Manifested in (1) by inserting partially constant superposition  $\mu$ .

$m$  is a finite number, because  $r$  ordinarily goes to zero as  $c\sqrt{x}$ . Then the product\*  $(r r')$  for small  $x$  is

$$r r' = \frac{c^2}{2};$$

that is, finite for  $x \rightarrow 0$  and equal to the radius of the curved sphere for point  $x = 0$ ,  $r = 0$ .

A different method of visualizing the dipolar intensities is to cut the solid parallel to its axis and perpendicular to the parallel flow and stipulate that the flow through the outside of this section, generated by the dipolar motion be equal to the flow of the undisturbed stream through this area, i.e., equivalent to the section multiplied by the flow velocity at infinity. It is not advisable to effect  $n$  such cuts to define the  $n$  dipolar intensities, because the slender forms of interest to us render the exact graphic analysis of the section difficult and at the same time becloud the dipolar effect when the cut is made at a distance  $r$  contiguous to  $r_{\max}$  from the axis. But it is advantageous to occasionally replace one or two equations with such flow conditions in the system (2).

The length of the constant dipolar intensities must be decided at the very beginning. Knowing  $\mu$  to be about proportional to  $r^2$ , according to Von Karman, the length of the <sup>interval</sup> spaces depends on the <sup>rate</sup> intensity of the change of  $r$ . It will be less toward bow and stern. The major obstacle lies in the choice of the starting point of the superposition, whose distance from the bow may be assumed  $x_1$ . For the sphere the ratio of  $x_1$  to curvature radius  $m$  is = 1. Long extended bodies having on the axis a stronger dipolar motion, the interference velocities outside of the body increase conformably to the flow condition, which means a shortening of distance  $x_1$ . Consequently, the starting point must be ahead of the center of curvature of the bow; for the rest, its selection must be left to experiment.

If a calculation is made first it affords a check on whether or not point  $x_1$  has been correctly chosen. If the surface of the body is really a surface of flow then even the higher differential quotients  $r''$ , etc., of the

---

\*  $(r r') = -\frac{d}{dx} \left( \frac{r^2}{2} \right)$ ; that is,  $r r'$  = the derivative of the curve  $\pi r^2(x)$  divided by  $2\pi$ .

meridian section of the closed stream surface, produced by superposed dipolar and parallel flow, must correspond with those of the surface of the body. We shall see whether this is the case for the bow. Differentiate equation (1) ~~with respect to~~ according to  $x$  and form the limit for  $x = 0$  and  $r = 0$ . Putting

$$\theta_{pv} = \frac{1}{p} \left( \frac{1}{\xi_p^{p+1}} - \frac{1}{\xi_p^p} \right) \quad (8)$$

and

$$\lim_{\substack{x \rightarrow 0 \\ r \rightarrow 0}} [(r'^2 + r r'') - 1] = 8$$

it manifests

$$\sum_{v=1}^n \mu_v \{ 5 \theta_{3v} + 7 m \theta_{4v} - 5 m^2 \theta_{5v} \} = 0 \quad (9)$$

The condition is extremely sharp. It shows that even a minor error in the selection of  $x_1$  is immediately followed by a tangible deviation from zero at the right side. Even an estimate of the anticipated  $\mu$  values may, under certain circumstances afford a check on the fulfillment of this condition. The  $\theta_{pv}$  values drop very quickly, so that for the balance only the first spaces come into consideration.

The speedy abatement of the  $\theta_{pv}$  values with rising  $p$  induces the following: Assuming that very high ~~derivatives~~ <sup>derivatives</sup> of the bulkhead surface curve are known, it would be possible to compute  $\mu_1$  directly by repeating differentiation of equation (1) and formation of its limit for  $x = 0$ ,  $r = 0$ , after having proceeded far enough so that  $\theta_{pv}$  abates rapidly, so that  $\mu_1$ , the first term of the sum, only, need be considered.

Now the course of the dipolar motion for pointed stern must be included yet. How close to the tip is the superposition to extend? It is readily shown that integral equation (1)

$$\begin{aligned} - \int_0^l \frac{\mu(\xi) d\xi}{\sqrt{r^2 + (x - \xi)^2}^3} + 3 r^2 \int_0^l \frac{\mu(\xi) d\xi}{\sqrt{r^2 + (x - \xi)^2}^5} - \\ - 3 r r' \int_0^l \frac{\mu(\xi) (x - \xi) d\xi}{\sqrt{r^2 + (x - \xi)^2}^5} = 4 \pi W, \end{aligned}$$

which the dipol motion must fulfill, affords no positive solution at the right of the maximum section for  $r, r' = 0$ , which begins in  $x = l, r = 0$  as  $\mu(\xi) = c(l - \xi)^\lambda$ , where  $\lambda$  and  $c$  are positive figures. It means: the dipolar motion cannot reach the tip and dipolar motion results only in an approximated rounded-off stern. In a practical sense there is, of course, no exact tip, but merely a point of very high, but still finite curvature. The question of final point of the superposition then would, provided a certain roundness is desired, revert to the considerations made for the bow. But the superposition toward the stern will be so small that a minor variation in final point will have no effect on the total result (on the moment, for instance).

### B. Continuous, Partially Linearly Variable

#### Dipolar Superposition

For not very slender solids the dipolar superpositions defined according to the described method are very much contingent upon the chosen space division. (See figs. 5-8.) This fluctuation admittedly diminishes as the number of dipolar spaces increases. But for mathematical reasons a minimum number is desirable, in order to keep the order of the resolvable equation system low. These considerations were the reasons for assuming a continuous, partially linearly variable superposition in place of a partially constant dipolar motion. The result was, as proved by examples to be given elsewhere, quite satisfying.

Proceeding from the general equation (1) for flow adherence, we first develop the equation system. With

$$\mu(\xi) = a_v + b_v \xi \quad (10)$$

in the  $v$ th interval, which extends from  $\xi_v$  to  $\xi_{v+1}$  (fig. 4), equation (1) becomes

$$-\sum_{v=1}^n \int_{\xi_v}^{\xi_{v+1}} \frac{a_v + b_v \xi}{\sqrt{r^2 + (x - \xi)^2}} d\xi + 3r^2 \sum_{v=1}^n \int_{\xi_v}^{\xi_{v+1}} \frac{a_v + b_v \xi}{\sqrt{r^2 + (x - \xi)^2}} d\xi - 3rr' \sum_{v=1}^n \int_{\xi_v}^{\xi_{v+1}} \frac{(a_v + b_v \xi)(x - \xi)}{\sqrt{r^2 + (x - \xi)^2}} d\xi = 4\pi W$$

or, when writing

$$a_v + b_v \xi = (a_v + b_v x) - b_v (x - \xi)$$

$$\begin{aligned} \sum_1^n (a_v + b_v x) & \left[ - \int_{\xi_v}^{\xi_{v+1}} \frac{d\xi}{\sqrt{r^2 + (x - \xi)^2}^3} + 3r^2 \int_{\xi_v}^{\xi_{v+1}} \frac{d\xi}{\sqrt{r^2 + (x - \xi)^2}^5} - \right. \\ & \left. - 3rr' \int_{\xi_v}^{\xi_{v+1}} \frac{(x - \xi) d\xi}{\sqrt{r^2 + (x - \xi)^2}^5} \right] - \sum_1^n b_v \left[ - \int_{\xi_v}^{\xi_{v+1}} \frac{(x - \xi) d\xi}{\sqrt{r^2 + (x - \xi)^2}^3} + \right. \\ & \left. + 3r^2 \int_{\xi_v}^{\xi_{v+1}} \frac{(x - \xi) d\xi}{\sqrt{r^2 + (x - \xi)^2}^5} - 3rr' \int_{\xi_v}^{\xi_{v+1}} \frac{(x - \xi)^2 d\xi}{\sqrt{r^2 + (x - \xi)^2}^5} d\xi \right] = 4\pi W \quad (11) \end{aligned}$$

The integrals of the first sum on the left side appear by Von Karman on page 3; those of the second sum are readily evaluated. Multiplying the whole equation by  $r^2$ , yields

$$\begin{aligned} \sum_1^n (a_v + b_v x) [\Delta g_v + r' \Delta f_v] - \sum_1^n b_v r [-(\sin^3 \vartheta_{v+1} - \sin^3 \vartheta_v) + \\ + (\sin^3 \vartheta_{v+1} - \sin^3 \vartheta_v) + r' (\cos^3 \vartheta_{v+1} - \cos^3 \vartheta_v)] = 4\pi r^2 W \quad (12) \end{aligned}$$

For abbreviation, we write:

$$\Delta l_v = (\sin^3 \vartheta_v - \sin^3 \vartheta_{v+1}) - (\sin \vartheta_v - \sin \vartheta_{v+1}) \quad (13)$$

$$\Delta k_v = (\cos^3 \vartheta_v - \cos^3 \vartheta_{v+1}),$$

so that (12) becomes

$$\sum_1^n (a_v + b_v x) [\Delta g_v + r' \Delta f_v] + \sum_1^n b_v r [\Delta l_v + r' \Delta k_v] = 4\pi r^2 W \quad (14)$$

Carrying the simplification further,

$$\left. \begin{aligned} \Delta g_v + r' \Delta f_v &= I_v, \\ x(\Delta g_v + r' \Delta f_v) + r(\Delta l_v + r' \Delta k_v) &= II_v; \end{aligned} \right\} \quad (15)$$



Equation (14), which defines  $a_v$  and  $b_v$ , assumes the form

$$\sum_1^n (a_v I_v + b_v II_v) = 4 \pi r^2 W \quad (16)$$

The superposition begins in  $\xi_1$  with value  $c$ . Then

$$\left. \begin{aligned} a_1 &= c - b_1 \xi_1 \\ a_2 &= c + b_1(\xi_2 - \xi_1) - b_2 \xi_2 \\ &\dots\dots\dots \\ a_v &= c + b_1(\xi_2 - \xi_1) + b_2(\xi_3 - \xi_2) + \dots + b_{v-1}(\xi_v - \xi_{v-1}) - b_v \xi_v \end{aligned} \right\} \quad (17)$$

From (16) follows

$$\begin{aligned} c \sum_1^n I_v + b_1 \left\{ (\xi_2 - \xi_1) \sum_2^n I_v - \xi_1 I_1 + II_1 \right\} \\ + b_2 \left\{ (\xi_3 - \xi_2) \sum_3^n I_v - \xi_2 I_2 + II_2 \right\} \\ + \dots\dots\dots \\ + b_{n-1} \left\{ (\xi_n - \xi_{n-1}) I_n - \xi_{n-1} I_{n-1} + II_{n-1} \right\} \\ + b_n \left\{ \begin{array}{l} - \xi_n I_n + II_n \end{array} \right\} = 4 \pi r^2 W, \end{aligned} \quad (18)$$

which is the equation system for computing the  $(n+1)$  unknown factors  $c, b_1, \dots, b_n$ . For the point  $x = 0, r = 0$ , the relation with the notations of equation (8) is

$$\sum_1^n \left\{ a_v (\theta_{2v} - 3m\theta_{3v}) + b_v (\theta_{1v} - 3m\theta_{2v}) \right\} = 4\pi W \quad (19)$$

Putting

$$\left. \begin{aligned} \theta_{2v} - 3m\theta_{3v} &= III_v, \\ \theta_{1v} - 3m\theta_{2v} &= IV_v. \end{aligned} \right\} \quad (20)$$

reveals for point  $x = 0, r = 0$

It should be observed, when carrying out the calculation, that the functions  $g, f, k, l$  are the same for all bodies dependent on  $\frac{x - \xi}{r}$ ;\* or, in other words, construe  $k$  and  $l$  in addition to  $g$  and  $f$  as in the Karman method. The development of equations (18) and (21) takes somewhat longer than when assuming partially constant dipolar superposition, but the decidedly better results by less number of spaces compensates for this drawback.

. To illustrate the preceding expositions there follows a compilation of calculated dipolar superposition for bodies which in axial flow are to be substituted by simple singularities on their axis. The body contour is indicated and the computed dipolar superposition plotted in units of the superposition, which corresponds to an indefinitely long cylinder of diameter  $(2 R)$  of maximum cross section in a transverse flow. Designating the plotted values with  $\mu^e(\xi)$ , the dipol moment  $\mu(\xi)$  is given by

(W = rate of flow). The abscissas of the utilized control points are shown by X's.

\*The functions g, f, k, l were omitted here because of the limited space for the scale, and the comparative ease with which the functions can be plotted.

1. Figure 5: a body which is produced by a source and sink of absolutely equal yield in a flow parallel to its connecting line. The yield in relation to the axial rate of flow is so proportioned that the maximum diameter equals  $1/5$  of the distance of the singularities. Bow and stern have the same shape, so the bow is shown only. It is readily apparent from Figure 5 that the starting point of the superposition was chosen too far away from the bow. As a result of its too remote distance from the bow the superposition of the first spacing is very large and, in order to neutralize its effects on the other parts of the contour, a negative superposition must ensue.

2. Figure 6: body produced as in Figure 5; yield of source and sink such as to make the maximum diameter equal the spacing of the singularities.

- a) The number of dipolar spacings is insufficient.
- b) and c) Partially linearly variable steady dipolar superposition assumed. In case c) it stipulates compliance with differentiated limiting conditions (compare page 5). Note that the fluctuations of the superposition in a) are perfectly in accord with rate of superposition b), c).

3. Figure 7: Fuhrmann (reference 2) shape No. IV. (The sketch shows the source distribution producing the body in axial flow.) The minor negative dipolar superposition adjacent to the bow is most probably due to not quite exact selection of starting point of superposition.

Fig. 4. Fuhrmann shape No. 1. This body has a very blunt nose. The dipolar superposition is computed in three ways. Because of the slight effect of nose and stern in very slender bodies the dipol superposition can, so to speak, be effected for two semi-bodies\*. For this body the dipol superposition, computed according to Von Karman's method, manifests unusual fluctuations at the bow (a). For that reason the equations, given by the postulated adherence of flow in the first two control points, were replaced by two flow conditions, which abated the fluctuations very materially (b). In Figure 8c the starting point is much farther away from the nose which, being very

---

\*The minor mutual effect can be accounted for by iteration.

blunt, causes the same phenomena as in example 2.

As concerns bodies with blunt nose, the iteration of the partial equation system for the nose is impossible.

## II. SUPERPOSITION ON THE SURFACE

### A. Development of Integral Equation for Surface Superposition and Its Reduction to a Unidimensional Integral Equation

The hesitation voiced at the beginning of this report against substituting for the body a dipol superposition on the axis, added to the experience gained by computing the cited examples, induced me to apply a different method for defining the potential  $\Phi$  of the transverse flow around a solid of rotation. Using the same notations as before, namely,  $x$  = axis of body,  $z$  = negative direction of parallel flow, which is perpendicular to  $x$ , and  $y$  = direction perpendicular to  $x$  and  $z$ , the potential  $\Phi$  is defined as follows: It must satisfy the potential equation  $\Delta\Phi = 0$ , it must act at infinity as  $(-Wz)$ , and on the surface of the body  $\frac{\partial\Phi}{\partial n}$  must be  $= 0$  ( $n$  = direction of the outside normal). Then resolve  $\Phi$  into  $\Phi_1$  and  $\Phi_2$ , where  $\Phi_1 = -Wz$ . On the surface  $\frac{\partial\Phi_1}{\partial n} = -W \frac{\partial z}{\partial n}$ . This fulfills the conditions for  $\Phi$ .  $\Phi_2$  must disappear at infinity and the normal ~~derivative~~ on the surface is  $\frac{\partial\Phi_2}{\partial n} = +W \frac{\partial z}{\partial n}$ .

The problem thus resolves to defining  $\Phi_2$ . This potential was approximated in the Rankine-Von Karman method by the dipol superposition of the body axis. But, conformably to the theory of mass potentials,  $\Phi_2$  can equally be represented as potential of an elementary source-sink superposition spread over the surface of the body. On the premise that the body everywhere has a ~~logically~~ defined tangential plane, that is, no cusps, this superposition can be expressed by (reference 3): (Goursat)

$$2\pi f(x,y,z) + \int_S f(\xi,\eta,\zeta) \frac{\cos\psi}{R^2} d\sigma = W \frac{\partial z}{\partial n} \quad (22)$$

Here  $S$ , surface of body.

$d\sigma$ , surface differential at point  $\xi, \eta, \zeta$ .

$\psi$ , angle between connecting line of fixed surface point  $P(x, y, z)$  and running point  $II(\xi, \eta, \zeta)$  with the normal in point  $P(x, y, z)$ . (Compare fig. 9.)

$R$ , distance of fixed from running point.

The body being symmetrical in rotation, cylindrical coordinates are introduced:

fixed point  $P$ :  $r = \sqrt{z^2 + y^2}$ ,  $z = r \cos \varphi_r$ ,  $x$ ,

running point  $II$ :  $\rho = \sqrt{\zeta^2 + \eta^2}$ ,  $\zeta = \rho \cos \varphi_\rho$ ,  $\xi$ , (23)

so that (22) becomes

$$2\pi f(x, r, \varphi_r) + \int_S f(\xi, \rho, \varphi_\rho) \frac{\cos \psi}{R^2} d\sigma = \frac{W \cos \varphi_r}{\sqrt{1 + \left(\frac{dr}{dx}\right)^2}} \quad (24)$$

In addition it is written  $\frac{dr}{dx} = r'$ ,  $\frac{d\rho}{d\xi} = \rho'$ . Extrapolation then yields from the geometrical relations shown in Figure 9,

$$\cos \psi d\sigma = + \frac{[r - r'(x - \xi)] - \rho \cos(\varphi_r - \varphi_\rho)}{R} \rho d\varphi_\rho d\xi \frac{\sqrt{1 + \rho'^2}}{\sqrt{1 + r'^2}} \quad (25)$$

and, with  $l$  = length of body,

$$2\pi f(x, r, \varphi_r) + \int_0^l \int_0^{2\pi} f(\xi, \rho, \varphi_\rho) \frac{[r - r'(x - \xi)] - \rho \cos(\varphi_r - \varphi_\rho)}{R^3} \rho d\varphi_\rho d\xi = \frac{W \cos \varphi_r}{\sqrt{1 + r'^2}} \quad (26)$$

which, abbreviated, yields:

$$\left. \begin{aligned} (x - \xi)^2 + r^2 + \rho^2 &= \alpha^2, \\ + 2 r \rho &= \kappa^2, \\ \varphi_r - \varphi_\rho &= \chi. \end{aligned} \right\} \quad (27)$$

So that

$$\begin{aligned} R^2 &= (x - \xi)^2 + r^2 + \rho^2 - 2 r \rho \cos(\varphi_r - \varphi_\rho) \\ &= \alpha^2 - \kappa^2 \cos(\varphi_r - \varphi_\rho) = \alpha^2 - \kappa^2 \cos \chi. \end{aligned}$$

It is readily seen that  $f(x, r, \varphi_r)$  must be proportional to  $W \cos \varphi_r$ . Consequently, with

$$f(x, r, \varphi_r) = f^e(x, r) W \cos \varphi_r,$$

a few changes result in

$$\begin{aligned} 2\pi f^e(x, r) + \int_0^{2\pi} \int_0^\infty f^e(\xi, \rho) \left[ \left\{ r - r' (x - \xi) \right\} \frac{\cos \chi}{\sqrt{\alpha^2 - \kappa^2 \cos \chi^2}} - \right. \\ \left. - \rho \frac{\cos^2 \chi}{\sqrt{\alpha^2 - \kappa^2 \cos \chi^2}} \right] \times \sqrt{\frac{1 + \rho'^2}{1 + r'^2}} \rho \, d\lambda \, d\xi \frac{1}{\sqrt{1 + r'^2}} \quad (28) \end{aligned}$$

In this integral equation the integration can be extended over  $\chi$ . It is necessary to define

$$J_1 = \int_0^{2\pi} \frac{\cos \chi}{\sqrt{\alpha^2 - \kappa^2 \cos \chi^2}} \, d\chi \quad (29)$$

and

$$J_2 = \int_0^{2\pi} \frac{\cos^2 \chi}{\sqrt{\alpha^2 - \kappa^2 \cos \chi^2}} \, d\chi \quad (30)$$

These integrations lead, after a number of transformations, to elliptical integrals. Putting (reference 4)

$$\tan \frac{\chi}{2} = t, \quad \cos \chi = \frac{1 - t^2}{1 + t^2}, \quad d\chi = \frac{2 \, dt}{1 + t^2}$$

and abbreviating,

$$\lambda^2 = \frac{\alpha^2 - \kappa^2}{\alpha^2 + \kappa^2},$$

yields

$$J_1 = \frac{4}{\sqrt{\alpha^2 + \kappa^2}^3} \left[ - \int_0^\infty \frac{dt}{\sqrt{1+t^2} \sqrt{\lambda^2 + t^2}} + \frac{2\alpha^2}{\alpha^2 + \kappa^2} \int_0^\infty \frac{dt}{\sqrt{1+t^2} \sqrt{\lambda^2 + t^2}^3} \right],$$

$$J_2 = \left( \frac{\alpha^4}{\kappa^4} \frac{4}{\sqrt{\alpha^2 + \kappa^2}^3} - \frac{8\alpha^2}{\kappa^4 \sqrt{\alpha^2 + \kappa^2}} \right) \int_0^\infty \frac{dt}{\sqrt{1+t^2} \sqrt{\lambda^2 + t^2}} \\ + \frac{4(1-\lambda^2)}{\sqrt{\alpha^2 + \kappa^2}^3} \frac{\alpha^4}{\kappa^4} \int_0^\infty \frac{dt}{\sqrt{1+t^2} \sqrt{\lambda^2 + t^2}^3} + \frac{4\sqrt{\alpha^2 + \kappa^2}}{\kappa^4} \int_0^\infty \frac{dt \sqrt{\lambda^2 + t^2}}{\sqrt{1+t^2}^3}$$

Moreover, the introduction of

$$t^2 = \lambda^2 \frac{\tau^2}{1 - \tau^2} \quad \text{and} \quad \kappa^2 = 1 - \lambda^2$$

results, when  $K$  denotes the complete elliptic normal integral of the first category, and  $E$  that of the second, in

$$J_1 = \frac{4}{\kappa^2 \sqrt{\alpha^2 + \kappa^2}} \left[ \frac{\alpha^2}{\alpha^2 - \kappa^2} E(k^2) - K(k^2) \right],$$

$$J_2 = \frac{\alpha^2}{\kappa^2} J_1 + \frac{4}{\kappa^4 \sqrt{\alpha^2 + \kappa^2}} [(\alpha^2 + \kappa^2) E(k^2) - \alpha^2 K(k^2)].$$

For the sake of simplicity, we put

$$J_1 = \frac{4}{\kappa^2 \sqrt{\alpha^2 + \kappa^2}} G_1(k^2), \quad (29a)$$

$$J_2 = \frac{4}{\kappa^2 \sqrt{\alpha^2 + \kappa^2}} [G_1(k^2) + G_2(k^2)], \quad (30a)$$

that is,

$$G_1(k^2) = \frac{\alpha^2}{\alpha^2 - k^2} E(k^2) - K(k^2) = \frac{1}{2} \frac{2-k^2}{1-k^2} E(k^2) - K(k^2) \quad (31)$$

$$\begin{aligned} G_2(k^2) &= \frac{2\alpha^2 + k^2}{k^2} E(k^2) - \frac{2\alpha^2 - k^2}{k^2} K(k^2) \\ &= 2 \frac{\alpha^2}{k^2} \{E(k^2) - K(k^2)\} + \{E(k^2) + K(k^2)\} \\ &= 2 \frac{2-k^2}{k^2} \{E(k^2) - K(k^2)\} + \{E(k^2) + K(k^2)\} \quad (32) \end{aligned}$$

Then (28) becomes

$$\begin{aligned} 2\pi f^e(x, r) + \frac{2}{r} \int_0^l f^e(\xi, \rho) \frac{1}{\sqrt{\alpha^2 + k^2}} \{G_1(k^2) [-r'(x-\xi) + (r-\rho)] - \rho G_2(k^2)\} \\ \times \sqrt{\frac{1+\rho'^2}{1+r'^2}} d\xi = \frac{1}{\sqrt{1+r'^2}} \quad (33) \end{aligned}$$

In this manner the two-dimensional integral equation (22) has been reduced to a unidimensional one, with nucleus or core:

$$\begin{aligned} \underline{K}(x, r; \xi, \rho) &= \frac{2}{r} \frac{1}{\sqrt{\alpha^2 + k^2}} \{G_1(k^2) [-r'(x-\xi) + (r-\rho)] - \\ &\quad - \rho G_2(k^2)\} \sqrt{\frac{1+\rho'^2}{1+r'^2}} \quad (34) \end{aligned}$$

This core  $\underline{K}$  is examined more closely. It contains the functions  $G_1(k^2)$  and  $G_2(k^2)$ , which are aggregates of <sup>complete</sup> whole elliptic normal integrals. Both become infinite for  $k^2 \rightarrow 1$ . Therefore, it is necessary to examine the behavior of the core in the vicinity  $k^2 = 1$  more closely. Conformably to the assumptions made previously, a regular fixed point  $x, r$  is stipulated (points  $x = 0, r = 0$  and  $x = l, r = 0$  are excluded for the time being). The term

$$k^2 = 1 - \lambda^2 = 1 - \frac{\alpha^2 - k^2}{\alpha^2 + k^2}$$



goes, when denoting  $(\xi - x)$  by  $\xi^e$ , toward 1 as  $1 - \epsilon^2 \xi^{e^2}$ , where  $\epsilon^2 = \left(\frac{1 + r'^2}{4 r^2}\right)$ , so long as  $4 r^2 \gg \xi_{\max}^{e^2}$ . The term  $[-r'(x - \xi) + (r - \rho)]$  goes toward 0 as  $-\frac{r''}{2} \xi^{e^2} \dots$

Since  $K(k^2)$  for  $k^2 \rightarrow 1$  goes infinite (reference 5) as  $-\left[\ln \frac{\sqrt{1 - k^2}}{4}\right]$ ,  $E(k^2)$  remains finite, and  $[\lim_{k^2 \rightarrow 1} E(k^2) = 1]$ , it is

$$\left. \begin{aligned} \lim_{k^2 \rightarrow 1} G_1(k^2) [-r'(x - \xi) + (r - \rho)] &= \frac{-r''}{4 \epsilon^2} = \frac{-r'' r^2}{1 + r'^2} \\ \text{and } \lim_{k^2 \rightarrow 1} \rho G_2(k^2) &= \lim_{k^2 \rightarrow 1} \rho \left[ 3 + \ln \frac{\sqrt{1 - k^2}}{4} \right] \end{aligned} \right\} \quad (35)$$

Thus, core  $\underline{K}(x, r; \xi, \rho)$  goes for  $k^2 \rightarrow 1$  or  $\xi^e \rightarrow 0$  to infinity as  $\ln \frac{\epsilon |\xi^e|}{4}$ , that is, it is integrable.

For the points  $x = 0, r = 0$  and  $x = l, r = 0$   $k^2(\xi^e)$  is 0, as far as point  $\xi = 0$  or  $\xi = l$  itself, where  $k^2 = 1$ ; that is,  $\underline{K}(x, r; \xi, \rho) = 0$  for all points outside of the fixed point. Consequently, the integral

$$\int_0^l \underline{K}(x, r; \xi, \rho) f^e d\xi$$

vanishes for these points. The stern of an airship is usually pointed, obviating the necessity of deliberating whether the limitation imposed previously can be removed; but, as a matter of fact, it cannot. (Reference 6) From the practical point of view this is of no significance, since the stern of an airship has no mathematically exact tip, but merely a point of very pronounced but withal finite curvature.

Thus, abbreviated, as on the preceding page, the integral equation becomes

$$2\pi f^e(x, r) + \int_0^l f^e(\xi, \rho) \underline{K}(x, r; \xi, \rho) d\xi = \frac{1}{\sqrt{1 + r'^2}} \quad (36)$$

\*The subscript "max" is to indicate the maximum for  $\xi^e$  at which the interpolation formula is still valid.

$$\text{or } f^e(x, r) = \frac{1}{2\pi} \frac{1}{\sqrt{1+r^2}} - \frac{1}{2\pi} \int_0^l f^e(\xi, \rho) \underline{K}(x, r; \xi, \rho) d\xi \quad (37)$$

To resolve it, the well-known iteration method is expedient. Choose as 0th approximation

$$f_0^e(x, r) = \frac{1}{2\pi \sqrt{1+r^2}},$$

define with this  $f_0^e$  the integral

$$f^e \underline{K} d\xi \approx \int_0^l f_0^e \underline{K} d\xi$$

and thus compute the first approximation  $f_1^e$ . The insertion of this value into the integral yields the second approximation, etc. The convergence of the method is assured (reference 7), because  $f_0^e(x, r)$  is finite, nucleus  $\underline{K}(x, r; \xi, \rho)$  is logarithmically infinite at one point only and  $\frac{1}{2\pi}$  is less than 1;  $f^e(x, r)$  is given by a series of rising powers of  $1/\pi$ . ~~It becomes~~ When

$$\underline{K}(x, r; \xi, \rho) = \frac{2}{r \sqrt{1+r^2}} \sqrt{1+\rho^2} \underline{K}^e(x, r; \xi, \rho) \quad (38)$$

and

$$P_n(x, r) = \int_0^l \frac{P_{n-1}(\xi, \rho)}{\rho} \underline{K}^e(x, r; \xi, \rho) d\xi \quad (39)$$

is initially put\* with

$$P_1(x, r) = \int_0^l \underline{K}^e(x, r; \xi, \rho) d\xi \quad (40)$$

then

$$f^e(x, r) = f_0^e(x, r) - \frac{f_0^e(x, r)}{r} \left[ \frac{P_1(x, r)}{\pi} - \frac{P_2(x, r)}{\pi^2} + \frac{P_3(x, r)}{\pi^3} - + \dots \right] \quad (41)$$

\*For  $r = 0$ , see preceding page.

## B. The Practical Solution of the Integral Equation

a) Numerical definition of core function.— The most time-consuming part of the solution is the definition of the nucleus or core  $\underline{K}^0(x, r; \xi, \rho)$  for different fixed points  $(x, r)$  of the body. The functions  $G_1(k^2)$  and  $G_2(k^2)$  being aggregates of whole elliptic normal integrals, are so plotted against  $k^2$ , as to be accessible. It should be remembered that both functions  $\rightarrow \infty$  for  $k^2 \rightarrow 1$ .  $G_2(k^2)$  becomes logarithmically infinite, that is, comparatively inferior to  $G_1(k^2)$ , which approaches infinity as  $\frac{1}{1 - k^2}$ . For more exact reading, it is therefore advisable to plot the function  $H(k^2) = (1 - k^2)G_1(k^2)$  for  $k^2$  values contiguous to 1, which remains finite for  $k^2 \rightarrow 1$ . Then mark off  $H(k^2)$  for a predetermined  $k^2$  and divide this value by  $(1 - k^2)$ , which yields

$$G_1(k^2) = \frac{H(k^2)}{1 - k^2}$$

Figures 10, 11, and 12 show the course of  $G_1(k^2)$ ,  $H(k^2)$  and  $G_2(k^2)$ . The calculus for a predetermined body then begins with the determination of the "form factor"  $k^2(x, r; \xi, \rho)$  for a fixed point  $(x, r)$  (fig. 13):

$$k^2(x, r; \xi, \rho) = 1 - \frac{\alpha^2 - k^2}{\alpha^2 + k^2} = 1 - \frac{(x - \xi) + (r - \rho)^2}{(x - \xi) + (r + \rho)^2} = 1 - \frac{r_0^2}{r_u^2} \quad (42)$$

$k^2$  can be computed by measuring off the distances  $r_0$  and  $r_u$ . It was found, however, that the purely numerical determination takes about the same time and yields, of course, more accurate data, especially in proximity of  $(x, r)$ .

---

\*k is then written in the form of

$$k^2 = 1 - \frac{1 + \left(\frac{r - \rho}{x - \xi}\right)^2}{1 + \left(\frac{r + \rho}{x - \xi}\right)^2}$$

Without mathematical term given for the contour, the calculation of

$$Q(x, r; \xi, \rho) = [(r - \rho) - r'(x - \xi)]$$

offers serious obstacles.

This term  $Q$  stipulates very exact knowledge of the tangential direction  $r' = \frac{dr}{dx}$  (fig. 14), and of the second derivation  $r''$ , in order to define the limiting value  $Q G_1(k^2)$  for  $k^2 \rightarrow 1$ . In Figure 14  $Q$  corresponds to distance  $AP$ . It is readily apparent to what errors any inaccuracy in  $r'$  of say, 2 per cent, can lead on a long, slender body. The absolute error of  $Q$  grows proportionally to  $(x - \xi)$ . Of advantage is it that  $k^2$  is very small ( $G_1(k^2)$  also) for large  $(x - \xi)$ . In close proximity of  $x$ , however, - that is, for small  $(x - \xi)$ ,  $G_1(k^2)$  assumes very high values, so that relatively minor discrepancies in  $Q$  have a pronounced effect on

$$K(x, r; \xi, \rho) = \frac{2}{r} \frac{1}{r_u} \left\{ G_1 Q - \rho G_2 \right\} \sqrt{\frac{1 + \rho'^2}{1 + r'^2}}$$

because of the existing difference. If the meridian curve of the body is given empirically, a very careful determination of the first and second derivative of  $r$  is absolutely necessary. In a given case, it is necessary to again integrate\*  $r''$  and  $r'$  obtained by numerical differentiation, to ascertain whether the initial values  $r(x)$  are attained again - within the permissible limits. If it results in an inadmissible discrepancy  $\Delta r(x)$ , it is possible in most cases to approximate it by a simple algebraic function and in this manner effect the necessary corrections on  $r''$  and  $r'$ .

b) Treatment of point of discontinuity of the core.-  
After computing the core for a number of fixed points  $(x, r)$  the integral  $P_n(x, r)$  can be determined. The core being logarithmically infinite for  $\xi \rightarrow x$  or  $k^2 \rightarrow 1$ , integration is possible in interval  $\Delta \xi$  also, which contains  $x$ , provided  $f$  remains finite. Whereas the integration can be made graphically (or planimetrically)

---

\*The integration of empirical functions is admittedly much safer than the differentiations as calculation method.

outside of this interval, within this critical interval it must be achieved numerically. (Figure 15.) The plot shows the curve for  $\underline{K}(x, r; \xi, \rho)$ . Assume the graphic integration is made from 0 to  $x - \Delta x_l$  and from  $x + \Delta x_r$  to  $l$ . The choice need not necessarily be  $\Delta x_r = \Delta x_l$ , but for expediency, we assume it is, and express it as  $\Delta x$ . Then the integral

$$I = \int_{x-\Delta x}^{x+\Delta x} p_n(\xi, \rho) \underline{K}^e(x, r; \xi, \rho) d\xi \quad (43)$$

must be computed. Herein

$$\left. \begin{aligned} p_1(\xi, \rho) &= 1 && \text{for computing } P_1(x, r) \\ p_2(\xi, \rho) &= \frac{P_1(\xi, \rho)}{\rho} && \text{" " } P_2(x, r) \text{ etc.} \end{aligned} \right\} \quad (44)$$

For  $\underline{K}^e$  its value is written:

$$I = \int_{x-\Delta x}^{x+\Delta x} \frac{p_n(\xi, \rho)}{\sqrt{\alpha^2 + \kappa^2}} \left\{ G_1(k^2) [(r-\rho) - r'(x-\xi)] - \rho G_2(k^2) \right\} d\xi.$$

For  $\xi \rightarrow x$ ,

$$G_1(k^2) [(r-\rho) - r'(x-\xi)]$$

remains finite, as shown elsewhere; thus integral

$$L_1 = \int_{x-\Delta x}^{x+\Delta x} \frac{1}{\sqrt{\alpha^2 + \kappa^2}} p_n(\xi, \rho) G_1(k^2) [(r-\rho) - r'(x-\xi)] d\xi \quad (45)$$

can be graphically determined. There remains

$$L_2 = \int_{x-\Delta x}^{x+\Delta x} \frac{1}{\sqrt{\alpha^2 - \kappa^2}} p_n(\xi, \rho) \rho G_2(k^2) d\xi \quad (46)$$

Since  $G_2(k^2)$  approaches infinity as  $\ln \frac{\sqrt{1-k^2}}{4}$  when  $k^2 \rightarrow 1$ , we put

$$G_2(k^2) = N(k^2) + \frac{4-3k^2}{k^2} \ln \frac{\sqrt{1-k^2}}{4}$$

The function

$$N(k^2) = E(k^2) \frac{4-k^2}{k^2} - \left[ K(k^2) + \ln \frac{\sqrt{1-k^2}}{4} \right] \frac{4-3k^2}{k^2} \quad (47)$$

remains finite for  $k^2 \rightarrow 1$ . (Figure 16.)

Integral  $L_2$  resolves itself to

$$L_2 = L_{21} + L_{22} + L_{23};$$

with

$$L_{21} = \int_{x-\Delta x}^{x+\Delta x} \frac{1}{\sqrt{\alpha^2 + k^2}} p_n(\xi, \rho) \rho N(k^2) d\xi \quad (48)$$

and, taking into account that  $k^2 = \frac{4r\rho}{\alpha^2 + k^2}$ \*

$$L_{22} = \frac{1}{2\sqrt{r}} \int_{x-\Delta x}^{x+\Delta x} [p_n(\xi, \rho) - p_n(x, r)] \sqrt{\rho} \left( \frac{4-3k^2}{k} \ln \frac{\sqrt{1-k^2}}{4} \right) d\xi \quad (49)$$

and

$$L_{23} = \frac{p_n(x, r)}{2\sqrt{r}} \int_{x-\Delta x}^{x+\Delta x} \sqrt{\rho} \frac{4-3k^2}{k} \ln \frac{\sqrt{1-k^2}}{4} d\xi \quad (50)$$

$L_{21}$  and  $L_{22}$  are to be defined graphically. The integrant of  $L_{22}$  remains finite, provided  $p_n(\xi, \rho)$  is a continuous function. For expedient evaluation function

$$M(k^2) = \frac{4-3k^2}{k} \ln \frac{\sqrt{1-k^2}}{4} \quad (51)$$

is constructed. (Fig. 17.)

Integral  $L_{23}$  is numerically interpreted. Developing

$$\left. \begin{aligned} k^2 &= 1 - \epsilon^2 \xi^{e^2} + \gamma \xi^{e^3} + \dots \\ \rho &= r + r' \xi^e + r'' \frac{\xi^{e^2}}{2} + r''' \frac{\xi^{e^3}}{6} + \dots \end{aligned} \right\} \quad (52)$$

---

\*Follows from easy extrapolation of equation (42).

yields

$$\sqrt{\rho} \frac{4 - 3 k^2}{k} = \sqrt{r} (1 + \beta_1 \xi^e + \beta_2 \xi^{e^2} + \{\beta_3 \xi^{e^3} \dots\}) \quad (53)$$

where

$$\left. \begin{aligned} \beta_1 &= \frac{r'}{2r} \\ \beta_2 &= 3.5 \epsilon^2 + \left[ \frac{r''}{4r} - \frac{1}{8} \left( \frac{r'}{r} \right)^2 \right] \\ \beta_3 &= 3.5 \frac{r'}{2r} \epsilon^2 - 3 \gamma \end{aligned} \right\} \quad (54)$$

As a rule we stop after the term with  $\xi^{e^2}$  and use the term of the 3d order to estimate the error. Stopping after the terms of the 2d order manifests for  $L_{23}$  (50)

$$\begin{aligned} L_{23} &= \frac{p_n(x, r)}{2} \int_{x-\Delta x}^{x+\Delta x} (1 + \beta_1 \xi^e + \beta_2 \xi^{e^2}) \ln \frac{\epsilon |\xi^e|}{4} d\xi = \\ &= \Delta x p_n(x, r) \left[ \left( 1 + \frac{\beta_2}{3} \Delta x^2 \right) \ln \frac{\epsilon}{4} + (\ln \Delta x - 1) \right. \\ &\quad \left. + \frac{\beta_2}{3} \Delta x^2 (\ln \Delta x - \frac{1}{3}) \right] \end{aligned}$$

The inclusion of the terms of the 3d order in (52) would yield a correction of the order of

$$C_0 = \Delta x p_n(x, r) \frac{\gamma}{2\epsilon^2} \left( \beta_1 \frac{\Delta x^2}{2} + \beta_3 \frac{\Delta x^4}{5} \right)^*$$

In this manner a reference point is obtained for the selection of  $\Delta x$ .

c) Examples.— The development of the formulas for computing the surface superposition was followed by various illustrative examples in order to check the utility of the method:

1. By a solid of rotation produced at distance  $2r_{\max}$  by a source and a sink.

---

\*For computing this correction, we put

$$\ln \sqrt{1 - \frac{\gamma}{\epsilon^2} \xi^e} = - \frac{\gamma}{2\epsilon^2} \xi^e$$

2. By Fuhrmann body No. IV.

3. By Fuhrmann body No. 1.

The last was chosen because of its specially inconvenient aspect when computing the axial superposition.

The different approximations of the function of superposition  $f^0(x,r)$  have been reproduced in Figures 18-20. The convergence of the method is seen to be quite good. In example 1, the single correction has always the same prefix throughout the entire body length, so that the error caused by the alternating prefixes of the corrective terms (41) is readily estimated. The first correction, of course, produces the principal change in all bodies. Compared to the first calculation of the core, the determination of the higher approximations presents few obstacles. For examples 2 and 3, the corrections change the prefix along the body - an effect of the almost conical stern. This change in prefixes is by itself unfavorable for the convergence. However, it being superior for slender bodies to that of example 1, the significance of change in prefix is withal subordinate.

### C. Calculation of Flow

#### a) Tangential velocity on the surface of the body.-

In practice it is important to be able to compute the pressure on the surface of the body, which means that the velocity must be known at every point of the surface. The velocity is divided into its components - normal and tangential. The first, induced by the superposition of the parallel flow in direction of negative axis  $z$  over the source flow, is zero. The second is divided in a point  $(x,r,\varphi)$  into components  $w_1$  and  $w_2$  at right angles to one another. Component  $w_1$  clings to the parallel of latitude in direction of the tangent, component  $w_2$  in direction of the tangent of the meridian through point  $(x,r,\varphi)$ . (Fig. 21.)  $w_1$  is figured positive in direction of growing angle  $\varphi$ ;  $w_2$  is valid as positive when pointing from nose to stern. Now, let  $f^0(\xi,\rho)$  denote, as before, the surface superposition conjugated to velocity  $W = 1$ . It results for  $w_1$  and  $w_2$  in:



$$w_1 = W \sin \varphi \left[ 1 + \frac{4}{r \sqrt{1+r'^2}} \int_0^l \frac{f^e(\xi, \rho) \sqrt{1+\rho'^2}}{\sqrt{\alpha^2 + \kappa^2}} \times \frac{\rho}{\sqrt{\alpha^2 + \kappa^2}} G_3(k^2) d\xi \right] \quad (55)$$

where

$$G_3(k^2) = \frac{1}{k^2} \left\{ (2 - k^2) K(k^2) - 2 E(k^2) \right\} \quad (56)$$

(fig. 22) and

$$w_2 = W \cos \varphi \left\{ - \frac{r'}{\sqrt{1+r'^2}} + \frac{2}{r \sqrt{1+r'^2}} \times \int_0^l \frac{f^e(\xi, \rho) \sqrt{1+\rho'^2}}{\sqrt{\alpha^2 + \kappa^2}} \left[ (x - \xi) + r'(r - \rho) \right] \times G_1(k^2) - \rho r' G_2(k^2) \right] d\xi \right\} \quad (57)$$

$G_3(k^2)$  is logarithmically infinite, the integral in (55) therefore finite. Note, when evaluating the integral of (57) that, whereas  $G_2(k^2)$  is logarithmically infinite,  $G_1(k^2)$  is as\*  $\frac{1}{1-k^2} = \frac{1}{\epsilon^2 \xi^{e2}}$ . On the other hand, since

$$Q^e = (x - \xi) + r'(r - \rho) = - (1+r'^2) \xi^e - \frac{r''}{2} \xi^{e2} + \dots$$

changes its prefix for  $\xi^e = 0$ ,  $Q^e G_1(k^2)$  goes, when proceeding from the left on  $x$ , toward  $+\infty$ , and toward  $-\infty$  when approaching  $x$  from the right. The integral

$$\int_0^l \frac{f^e(\xi, \rho) \sqrt{1+\rho'^2}}{\sqrt{\alpha^2 + \kappa^2}} Q^e G_1(k^2) d\xi$$

must therefore be expressed by its "principal value"

---

\*  $\xi^e = \xi - x$ .

$$\lim_{\delta \rightarrow 0} \left[ \int_0^{x-\delta} \frac{f^e(\xi, \rho) \sqrt{1+\rho'^2}}{\sqrt{\alpha^2 + \kappa^2}} Q^e G_1(k^2) d\xi \right. \\ \left. + \int_{x+\delta}^l \frac{f^e(\xi, \rho) \sqrt{1+\rho'^2}}{\sqrt{\alpha^2 + \kappa^2}} Q^e G_1(k^2) d\xi \right]$$

Another point to be noted with  $w_2$  is that the integral for points  $x = 0, r = 0$  and  $x = l, r = 0$  does not disappear (in contrast to the normal component set up by source superposition alone). It is best to define the integral for this point separately, foregoing the reductions, which lose their significance because  $k^2$  is always zero up to one point. Tangential velocity  $\bar{w}_2$  set up in point  $x = 0, r = 0$  by source superposition is in direction of negative axis  $z$  and known in magnitude by (fig. 23)

$$\begin{aligned} |\bar{w}_2| &= 2W \int_{-\pi/2}^{+\pi/2} \int_0^l \frac{f^e(\xi, \rho) \cos \varphi \rho}{R^2} \sin \vartheta \sqrt{1+\rho'^2} d\xi \cos \varphi \rho d\varphi \\ &= 2W \int_0^l \frac{f^e(\xi, \rho) \rho^2 \sqrt{1+\rho'^2}}{R^3} d\xi \int_{-\pi/2}^{+\pi/2} \cos^2 \varphi \rho d\varphi \\ &= \pi W \int_0^l \frac{f^e(\xi, \rho) \rho^2 \sqrt{1+\rho'^2} d\xi}{R^3} \end{aligned} \quad (58)$$

wherein  $R = \sqrt{\xi^2 + \rho^2}$ .

b) The potential in any point of the space.— This is given by

$$\Phi = -4W \cos \varphi_r \int_0^l \frac{f^e(\xi, \rho) \sqrt{1+\rho'^2}}{\sqrt{\alpha^2 + \kappa^2}} G_3(k^2) \rho d\xi \quad (59)$$

$G_3(k^2)$  being the function defined by (56).

Note, that  $k^2 = 1 - \left(\frac{r_0}{r_u}\right)^2$  is always 1, when computing the potential in points outside of the body. As a result, no discontinuity places of the integrand appear.

## SUMMARY

An outline of Von Karman's method of computing the potential flow of airships in yaw by means of partially constant dipolar superposition on the axis of the body is followed by several considerations for beginning and end of the superposition. Then this method is improved by postulating a continuous, in part linearly variable dipolar superposition on the axis.

The second main part of the report brings the calculation of the potential flow by means of sources and sinks, arranged on the surface of the airship body. The integral equation which must satisfy this surface superposition is posed, and the ~~same~~<sup>kernel</sup> reduced to functions developed from whole elliptic normal integrals. The functions are shown diagrammatically. The integration is resolvable by iteration. The consequence of the method is good. The formulas for computing the velocity on the surface and of the potential for any point conclude the report.

Translation by J. Vanier,  
National Advisory Committee  
for Aeronautics.

## REFERENCES

1. Kármán, Th. v.: Calculation of Pressure Distribution on Airship Hulls. T.M. No. 574, N.A.C.A., 1930.
2. Fuhrmann, G.: Theoretische und experimentelle Untersuchungen an Ballonmodellen. Diss., Göttingen, 1912.
3. Heywood u. Fréchet: L'équation de Fredholm, pp. 17, 26, Paris, 1912.  
Goursat: Cours d'analyse mathématique, t. III, p. 281, Paris, 1923.
4. Serret-Scheffers: Lehrbuch der Differential- und Integralrechnung, Vol. II, p. 78 ff. Teubner, Leipzig, u. Berlin, 1911.
5. Jahnke-Emde: Funktionentafeln mit Formeln und Kurven, p. 52, Leipzig, 1928.
6. Poincaré, H.: Théorie du Potential Newtonien, p. 119, Paris, 1899.
7. Goursat: Cours d'analyse mathématique, Vol. III, p. 344 ff., Paris, 1923.

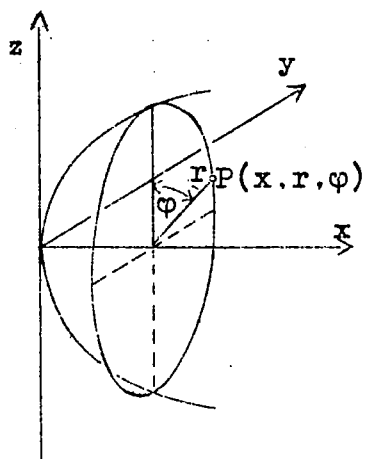


Fig. 1 Coordinate axes

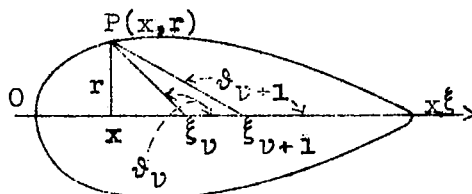


Fig. 3 Notations

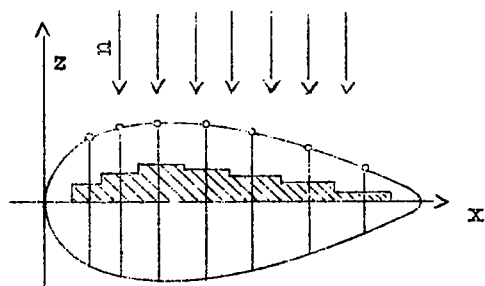


Fig. 2 Body with dipolar superposition on the axes.

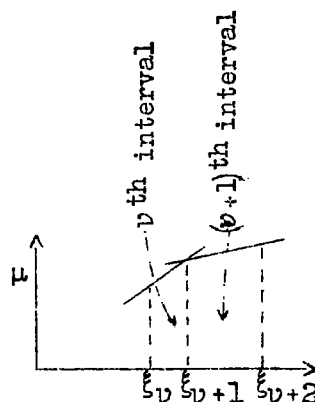


Fig. 4 Intervals by partially linearly variable dipolar superposition.

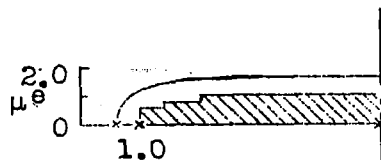


Fig. 5a

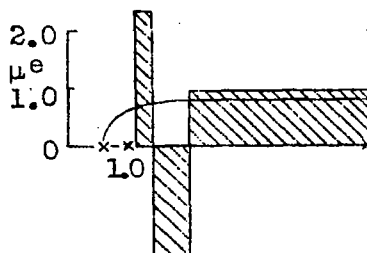


Fig. 5b

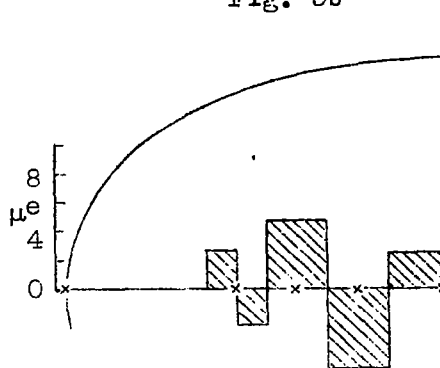


Fig. 6a

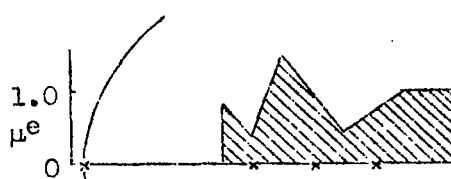


Fig. 6b

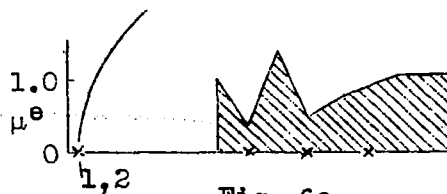


Fig. 6c

Figs. 5,6  
Computed  
dipolar  
superpositions

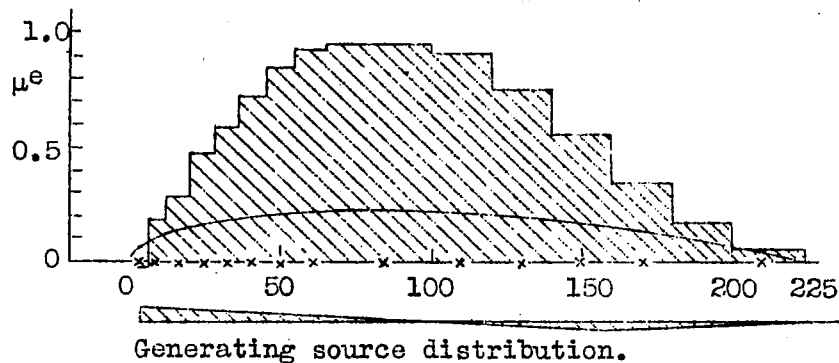


Fig. 7

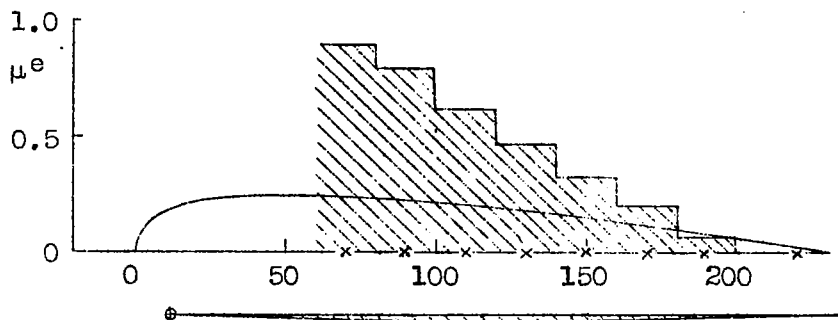


Fig. 8

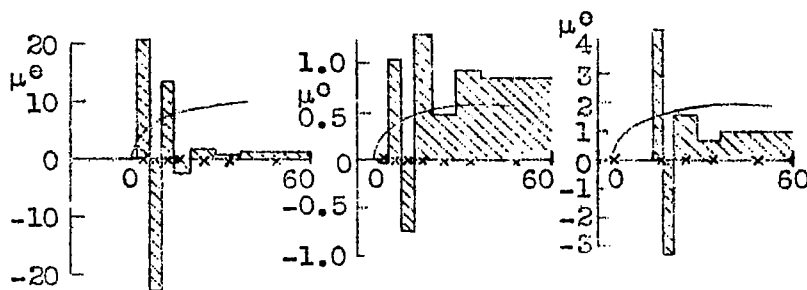


Fig. 8a

Fig. 8b

Fig. 8c

Figs. 7,8 Computed dipolar superpositions.

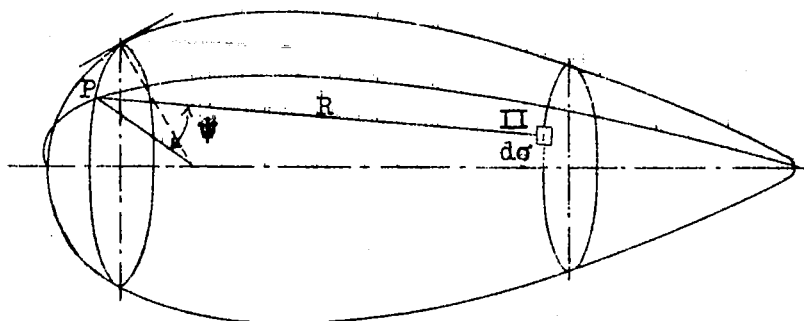


Fig. 9 Notations for surface superposition.

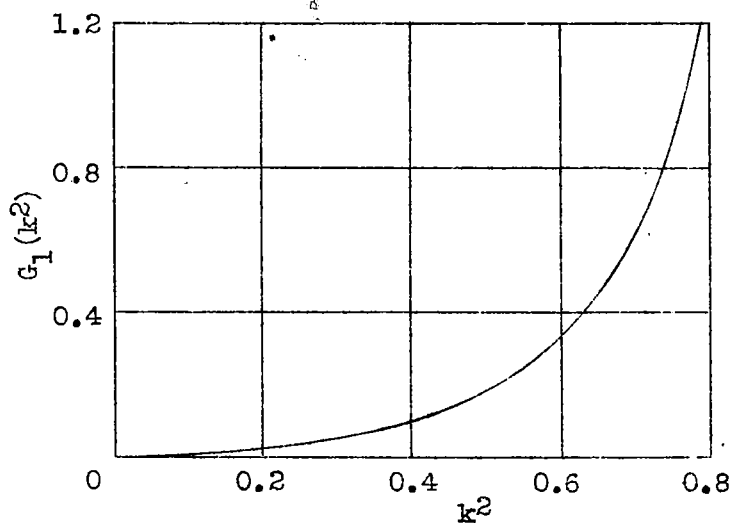


Fig. 10 The  $G_1(k^2)$  function.

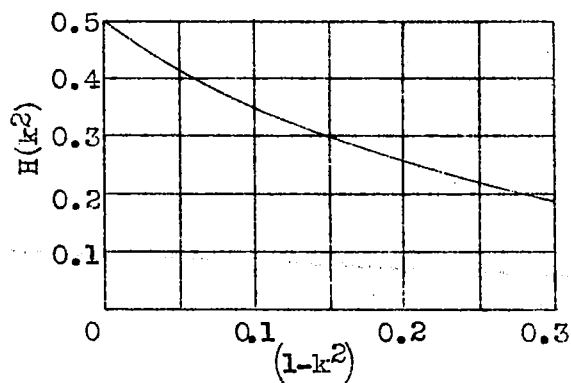


Fig. 11 The  $H(k^2) = (1-k^2)G_1(k^2)$  function.



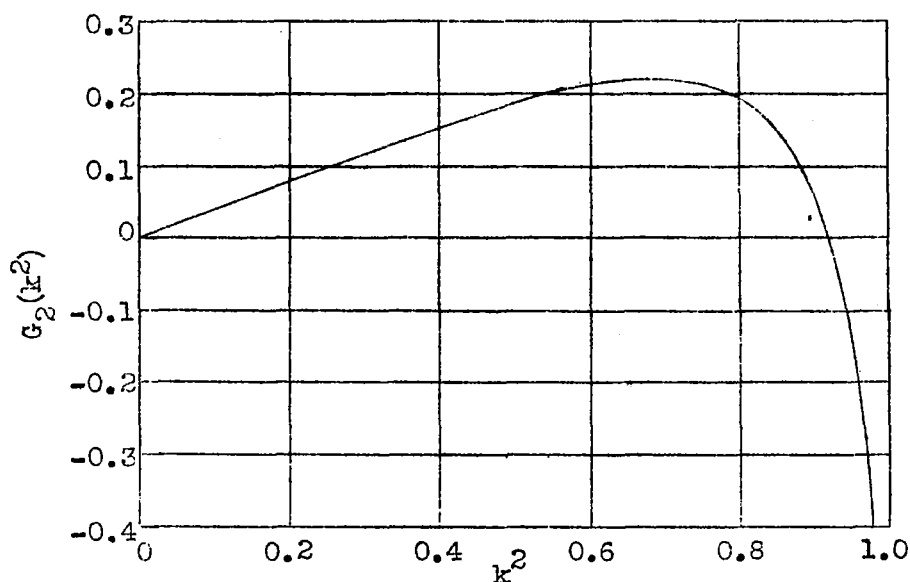


Fig. 12 The  $G_2(k^2)$  function.

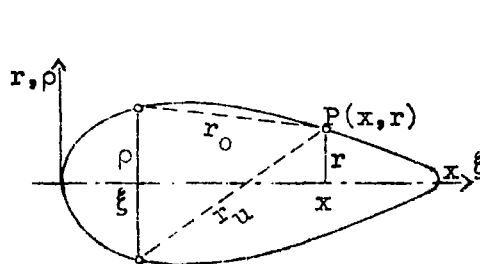


Fig. 13 Definition of form factor  $k^2$

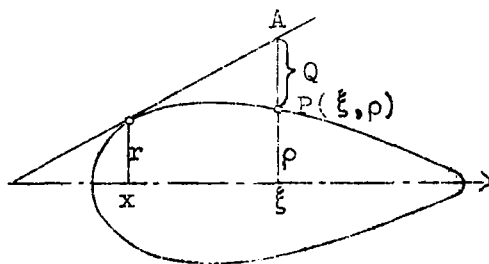


Fig. 14 Geometrical significance of  $Q$

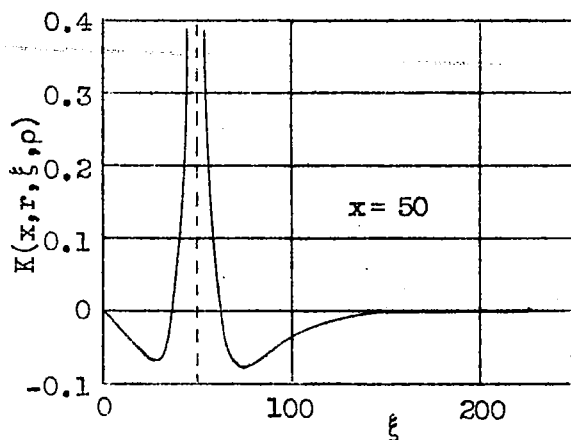


Fig. 15 Function of curve  $K(x, r, \xi, \rho)$  for  $x = 50$ . (Fuhrmann shape No.1,  $l = 230$ )

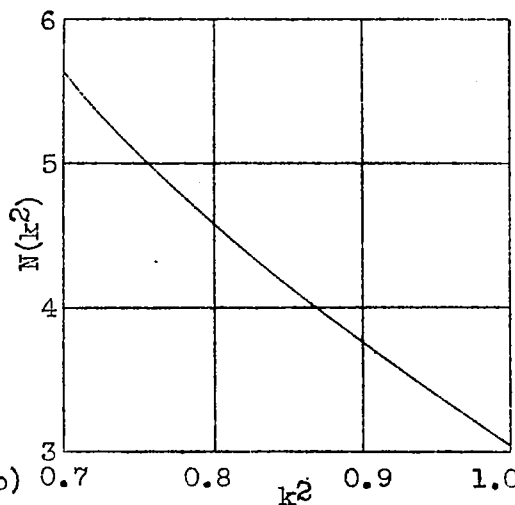


Fig. 16 The  $N(k^2)$  function.

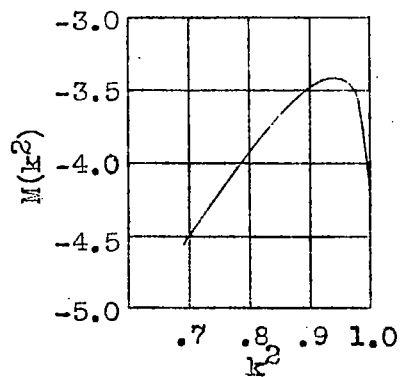


Fig. 17 The  $M(k^2)$  function.

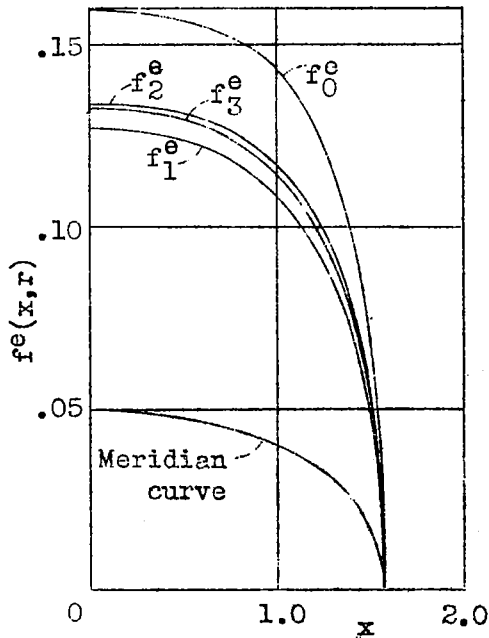


Fig. 18 Surface superposition of source - sink body.

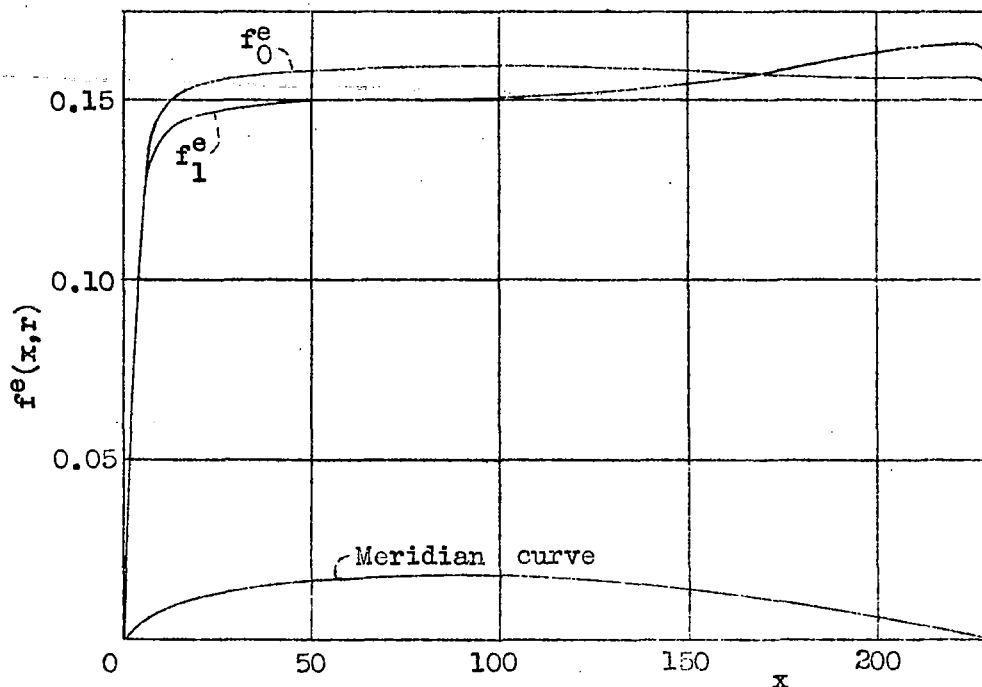


Fig. 19 Surface superposition of Fuhrmann shape No. IV

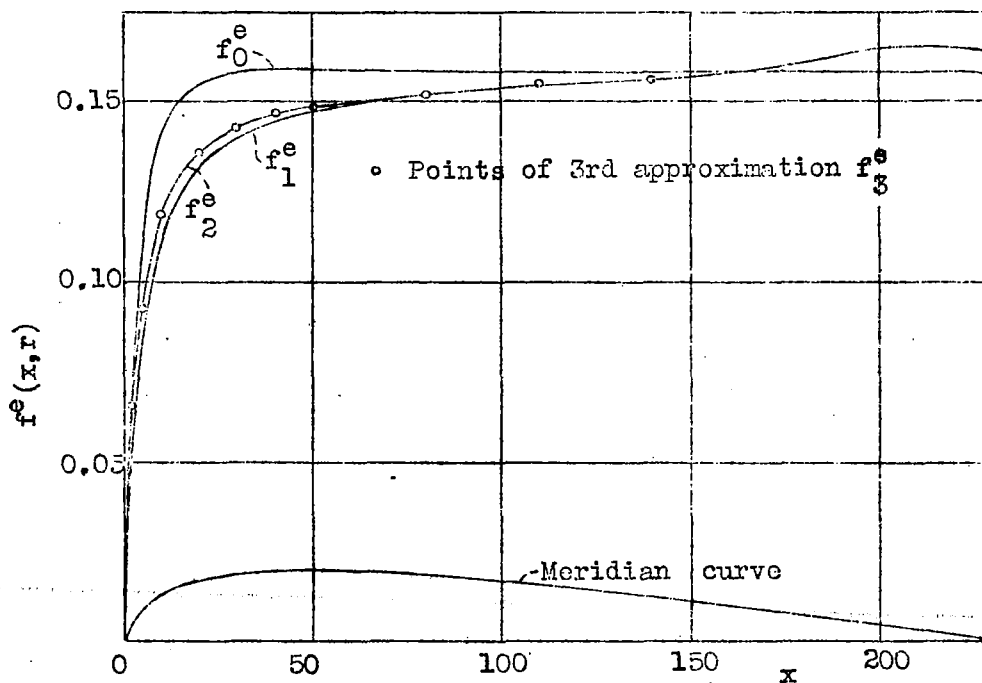


Fig. 20 Surface superposition of Fuhrmann shape No. I

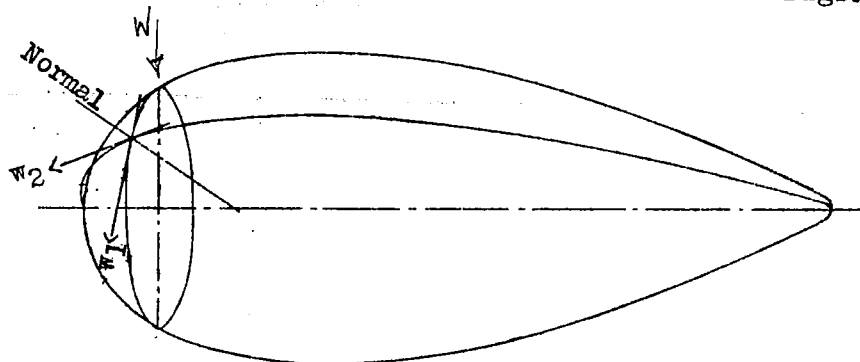


Fig. 21 Velocity components on surface of body.

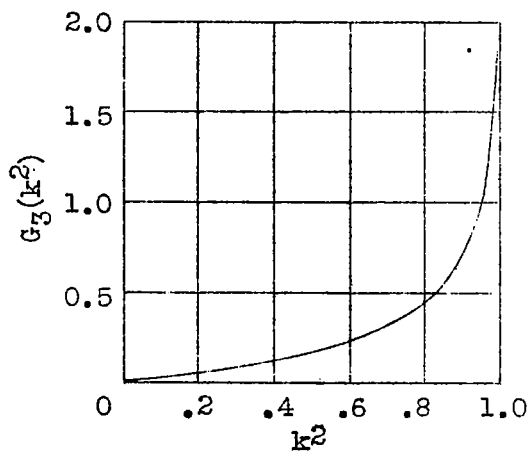


Fig. 22 The  $G_3(k^2)$  function

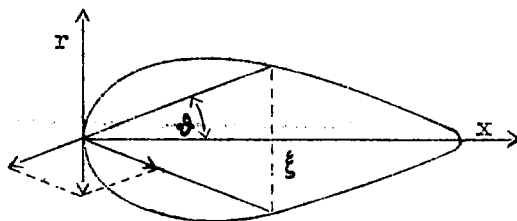


Fig. 23 Meridian cut at angle  $\phi$

LANGLEY RESEARCH CENTER



3 1176 01324 4315